Fluctuation of Heat Transfer in Shock Wave/Turbulent Boundary-Layer Interaction

Masanori Hayashi,* Shigeru Aso,† and Anzhong Tan‡
Kyushu University, Fukuoka, Japan

A new method for the measurement of heat-transfer rate with high spatial resolution and fast response is applied to the measurements of the fluctuating heat fluxes in the interaction regions of oblique incident shock waves and turbulent boundary layers. Experiments are performed under these testing conditions of Mach number of 4, wall temperature condition T_w/T_0 of 0.56, and Reynolds number of 1.26×10^7. Measurements are made for both unseparated and separated boundary-layer conditions. For the case of an unseparated boundary layer, fluctuations of heat flux become strong near the impingement point of the incident shock wave, and no intermittency phenomenon is observed. For the case of a separated boundary layer, significant fluctuations of heat flux are observed throughout the interaction region. These fluctuations are very strong, especially near the separation and reattachment points. Near the separation point, intermittency of heat transfer is observed.

Nomenclature

C_p = constant pressure specific heat
K_{qw} = Kurtosis coefficient of fluctuations of heat flux
M = Mach number
n = number of points used in calculating δ_{q_w}, etc.
p = pressure
Pr = Prandtl number
q_w = surface heat flux
r = recovery factor
S_{qw} = skewness coefficient of fluctuations of heat flux
St = Stanton number
T = temperature
U = velocity
X = streamwise distance from flat-plate leading edge
X_{imp} = streamwise distance from flat-plate leading edge to the inviscid shock wave impingement point
γ = intermittent factor
σ_{qw} = standard deviation of heat flux
ρ = density

Superscript

$(\bar{\ })$ = ensemble average

Subscripts

0 = undisturbed condition
aw = adiabatic wall condition
w = condition at wall
∞ = freesteam condition

Introduction

ONE of the serious problems in high-speed flight is the intensive aerodynamic heating in the interaction region of shock waves and turbulent boundary layers. From the early 1970's, extensive experimental investigations on aerodynamic heating caused by the interactions between shock waves and turbulent boundary layers have been conducted.[1-5] For practical design considerations, one of the most important phenomena is the appearance of large peak heating rates in the interaction regions. Because peak heating often occurs within a small length scale[6] and can have serious consequences, it is very important to reveal the detailed structure of aerodynamic heating in the interaction regions. However, because of the difficulties of experiments in high-speed flows and lack of proper heat-transfer measurement methods, the detailed features of aerodynamic heating in the interaction regions and the detailed structures of the flowfields are still unclear.

We have developed a new type of heat-flux sensor that has high spatial resolution and fast response and can be used in wind tunnels with long flow duration.[7] The theory of measurement, the method of manufacturing, and the calibration method for the new sensor have also been established. The principle of measurement is based on measuring the temperature gradient across a thin, heat-resistant layer with two thin-film resistance thermometers on its upper and lower surfaces. We have measured the distribution of heat-transfer coefficients in the interaction region with the sensor, and the complicated features of the aerodynamic heating in the interaction region have been revealed.[8]

Recently, many experimental investigations on the unsteadiness in the interaction regions are reported. Dolling and Murphy[9] measured the unsteadiness in the separated region of a compression corner and indicated an inherent character of oscillation of separation shock wave in the interaction regions. There are other observations about the unsteadiness in a variety of high-speed flows, such as over forward-facing steps[10] and past blunt fins and protuberances,[11] and in the shock impinging regions.[12] However, those experimental efforts were limited mainly to the pressure fluctuations. It is important to know the unsteady properties of surface heat flux in order to discover the structure of aerodynamic heating and to provide information for the improvement of turbulence modeling with heat-flux calculations.

With the high-frequency response and high spatial resolution of the multilayered heat-transfer gage, we have measured the fluctuations of surface heat flux in the interaction regions of the incident shock waves and turbulent boundary layers. Both the unseparated and separated cases are investigated. The results of these two cases show completely different tendencies in the interaction regions. In the unseparated case, the fluctuations grow strong only near the foot of the incident shock wave, and no intermittency is observed. In the separated

Received Dec. 16, 1987; presented as Paper 80-0426 at the AIAA 26th Aerospace Sciences Meeting, Reno, NV, Jan. 10-14, 1988; revision received May 5, 1988.

*Professor, Aeronautical Engineering. Member AIAA.
†Associate Professor, Aeronautical Engineering. Member AIAA.
‡Graduate Student, Aeronautical Engineering.

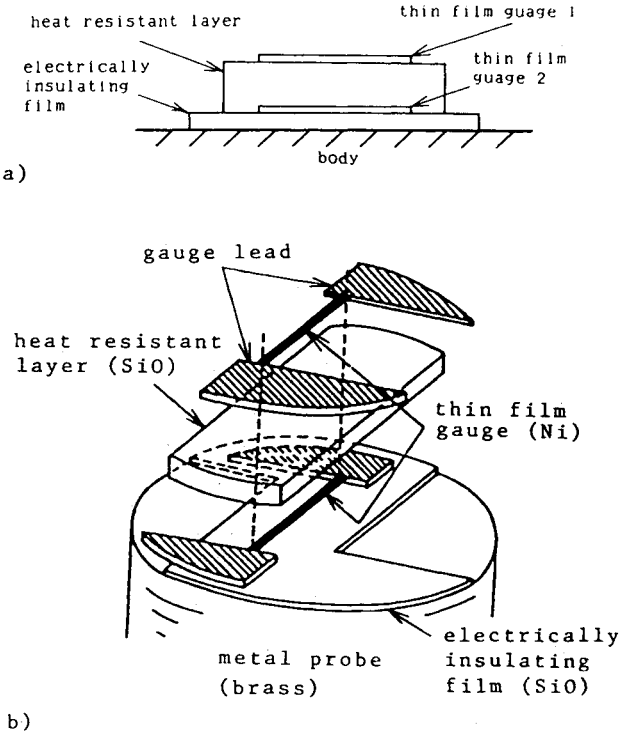

Fig. 1 a) Schematic and b) structure diagram of multilayered thin-film heat-transfer gage.

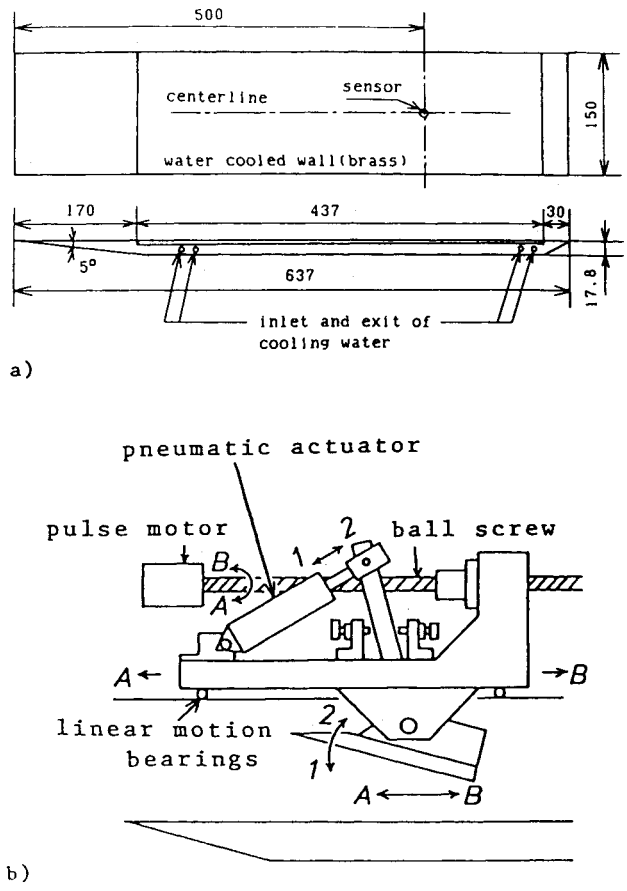

Fig. 2 a) Flat-plate model and b) shock generator.

case, the fluctuations are very strong throughout the interaction region and become significantly strong near the separation point and the reattachment point; intermittency in the fluctuations of heat flux is observed near the separation point. From a comparison of these results with those of the wall pressure fluctautions,[12] we have found that the fluctuations in heat flux have qualitatively the same features as those of the wall pressure but noticeable quantitative differences.

Multilayered Thin-Film Heat-Transfer Gage

Schematic diagrams of a multilayered thin-film heat-transfer gage and of the structure of the sensor are shown in Fig. 1. The principle of the measurement is based on measuring the temperature difference across the heat-resistant layer with two thin-film resistance thermometers on its upper and lower surfaces. These layers and films are deposited by the vacuum evaporation technique. SiO is used for the heat-resistant layer and the electrically insulating film, and Ni is used for thin-film gages and their leads. Two gages are connected to a bridge circuit, and the bridge outputs that are proportional to the temperature change are measured. For the calculation of heat flux from the bridge outputs, two calibration factors should be determined. By applying a step heat input to the sensor, a sensor can be calibrated easily and correctly. Details about the manufacture and the measurement devices and the calibration method for the sensor are described in Ref. 7.

The sensor used for the present experiments has thin-film gages 3 mm long and 0.2 mm wide. The sensitivity of the sensor is about 2.1×10^{-9} V/(W/m^2) for bridge voltage of 1 V. The response of the sensor for the step heat input has a rise time of about 0.5 ms.

Experimental Apparatus and Procedure

The Kyushu University supersonic wind tunnel with nominal Mach number of 4, test section of 150×150 mm, is used for the present experiments. The flat plate shown in Fig. 2a is placed parallel to the freestream. The plate is cooled by water to keep the wall temperature constant during the experiments. The sensor is set on the centerline of the plate 500 mm from the leading edge of the plate.

The boundary layer generated on the flat plate is used in experiments. Boundary-layer trips are not used. The Reynolds number based on the distance from the leading edge to the measuring point is about 1.26×10^7. Since boundary-layer transition occurs at a Reynolds number of about $3\text{–}5\times10^5$, the boundary layer at the measuring point is considered to be turbulent. The thickness of the boundary layer is about 7 mm, estimated from the visualization by the schlieren method. This value is almost the same as that estimated by conventional boundary-layer calculation.

The incident shock wave is induced by the full-span shock generator placed over the flat plate. The shock generator is designed to move longitudinally to enable a single sensor to scan the whole interaction region. To avoid choking at the starting of the wind tunnel, the shock generator is kept parallel to the freestream at first and then pitched up at a specified wedge angle after the wind tunnel has been started. For pitching and scanning operation of the shock generator, a pneumatic actuator and the combination of a ball screw and a pulse motor are used, respectively. The schematic diagram of the pitching and scanning mechanism of the shock generator is shown in Fig. 2b.

Two representative shock angles are selected so that both unseparated and separated cases can be studied. Test conditions are shown in Table 1.

The flowfields are also visualized using a surface oil-flow technique in order to check the two-dimensionality of the interaction. Surface oil-flow patterns show that the flowfields are essentially two-dimensional within the half-span of the plate.

In the experiments, the shock generator is moved along the freestream and stopped at the prescribed points, and the data are recorded. All of the movements of the shock generator and

Table 1 Test conditions

	Shock angle β, deg	Mach number M_∞	Total pressure $P_0, \times 10^6$ Pa	Total temperature T_0, K	Reynolds number $Re, \times 10^7$	Ratio of wall temperature to total temperature T_w/T_0
Unseparated case	18.5	3.82	1.24	540	1.26	0.56
Separated case	22.3	3.89	1.26	535	1.26	0.57

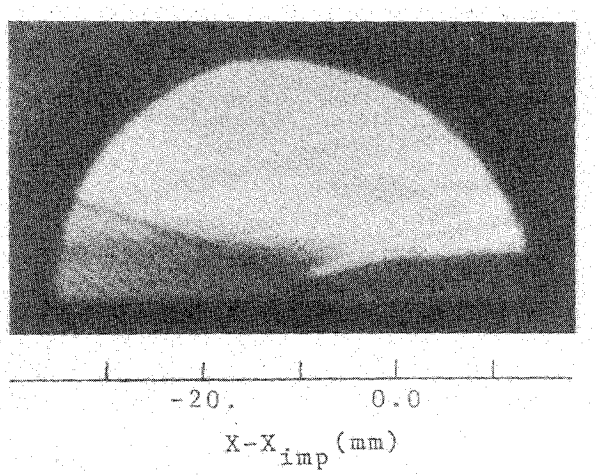

Fig. 3 Schlieren photograph of the unseparated interaction flowfield.

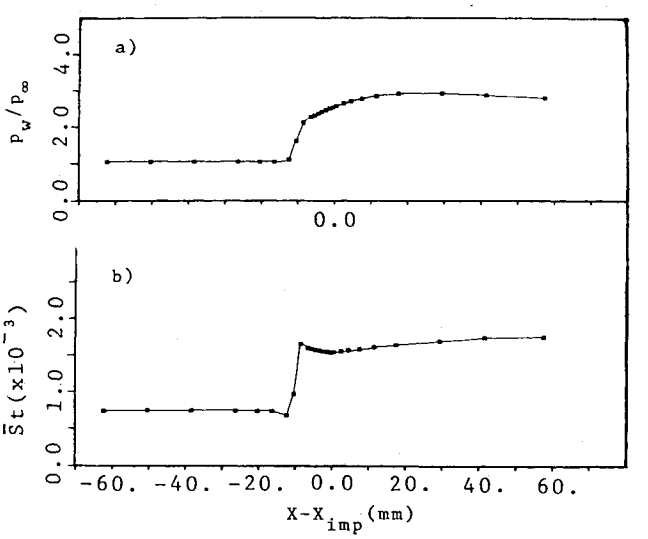

Fig. 4 a) Wall pressure and b) heat-transfer distribution in the unseparated interaction.

all data acquisition are controlled with microcomputers. Output from the sensor is amplified, filtered, and then recorded in a 10-bit A/D converter. The sampled data are stored imrate is set at 50 kHz, in view of the frequency response of the sensor. In each run, data are recorded at several 10-point intervals, and each record length is 2048 words. At each interval, especially where fluctuations of heat flux are severe, several samplings are conducted in order to get good convergence.

Results and Discussion

Wall pressure distributions are normalized with respect to the freestream static pressure values. Heat transfer to the wall is expressed as Stanton number. The Stanton number is calculated as follows:

$$\bar{St} = \bar{q}_w / \rho_\infty C_{p_\infty} U_\infty (T_{aw} - T_w) \tag{1}$$

where

$$T_{aw} = T_\infty \left(1 + r \cdot \frac{\gamma - 1}{2} M_\infty^2\right)$$

$$r = \sqrt[3]{Pr_w}, \quad Pr_w = Pr \quad \text{at} \quad T_w$$

The standard deviation of heat-flux fluctuation is expressed as

$$\sigma_{q_w} = \sum_{i=1}^{n} (q_{w_i} - \bar{q}_w)^2 \Big/ \sigma_{q_w}^2 \tag{2}$$

Higher-order moments of fluctuations, the skewness coefficient, and the Kurtosis coefficient are expressed as

$$\text{skewness coefficient} = \left[\frac{1}{n} \sum_{i=1}^{n} (q_{w_i} - \bar{q}_w)^3\right] \Big/ \sigma_{q_w}^3 \tag{3}$$

$$\text{Kurtosis coefficient} = \left[\frac{1}{n} \sum_{i=1}^{n} (q_{w_i} - \bar{q}_w)^4\right] \Big/ \sigma_{q_w}^4 \tag{4}$$

Unseparated Case

The flowfield of the unseparated interaction is visualized by the schlieren method as shown in Fig. 3. The incident shock wave penetrates deeply into the boundary layer and is reflected as a single shock wave. The incident shock wave bends in the boundary layer. Thus, the actual impingement point is somewhat upstream of that of the inviscid shock wave.

The wall pressure and the heat-transfer distribution in the interation region are shown in Fig. 4. The inviscid shock impingement point (X_{imp}), where the inviscid incident shock wave impinges at the wall, is taken as the origin of the streamwise coordinate ($X - X_{\text{imp}}$), and downstream is taken as positive. The reason to choose the inviscid shock impingement point as the origin is mainly the difficulty in determining the actual impinging point in the separated case, in which the incident shock wave could not reach to the wall. The actual impingement point of the shock wave in this case is about 10 mm upstream of the inviscid impingement point, namely, at $X - X_{\text{imp}} = -10$ mm.

The representative signals of the output from the heat-flux sensor are shown in Fig. 5. Positions at which the signals are recorded are also shown at the right-hand side of the figure. The signals are filtered by a low-pass analog filter with a cutoff frequency of 5 kHz. No digital filter is used. The noise level of the sensor is also shown at the bottom of the figure. The signal-to-noise ratios of the sensor outputs are about 5 in the undisturbed boundary layer and 20–100 in the interaction

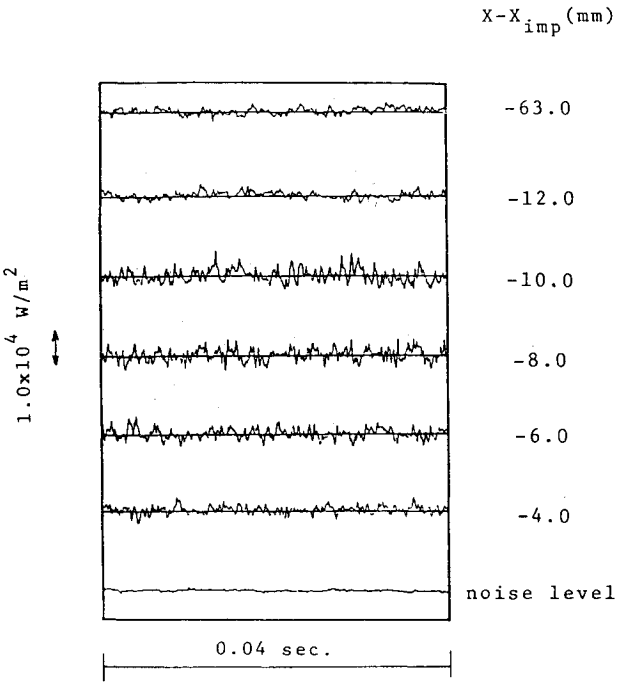

Fig. 5 Signals of the heat flux in the unseparated interaction.

region. Near the impinging point of the shock wave, the amplitude of the fluctuations of heat flux becomes large and then decays rapidly in the downstream. No intermittent signals of heat flux in this flowfield are observed.

The standard deviation normalized by mean heat flux is shown in Fig. 6a. Only a single peak is observed at the impinging point of the shock wave, and $\sigma_{qw}/\bar{q}_w$ is not increased downstream after the impingement of the shock wave. The higher-order moments are shown in Fig. 6b. No remarkable peaks in the distribution of these moments are observed. Both remain close to the Gaussian values. This indicates that the fluctuations of heat flux in the flowfield closely follow the Gaussian probability distribution. These results are qualitatively comparable with that of the wall pressure fluctuations.[12]

Separated Case

When the boundary layer is separated, the flowfield becomes quite complicated. The schlieren photograph of the separated interaction flowfield is shown in Fig. 7. A set of compression waves forms before the separation point. An expansion wave fan emanates from the point at which the incident shock wave reaches the boundary-layer edge over the separation region.

The distribution of mean wall pressure and of the Stanton number in the separated interaction region is shown in Fig. 8. The separation and reattachment points are indicated by S and R in the figure. The separation point, which is somewhat downstream of the first inflection point of the wall pressure distribution, is determined from the schlieren photograph. It is consistent with the results obtained by Green.[13] The reattachment point is indicated at the third inflection point of the wall pressure distribution, at about the same position determined from the schlieren photograph. The mean heat-transfer distribution has a peak near the separation point and increases after the reattachment point.

The representative signals of fluctuations of heat flux in the interaction region are shown in Fig. 9. Intermittency is observed near the separation point, and after the separation point turbulent fluctuations are observed.

The standard deviation normalized by mean heat flux is shown in Fig. 10a. The $\sigma_{qw}/\bar{q}_w$ shows a sharp peak near the

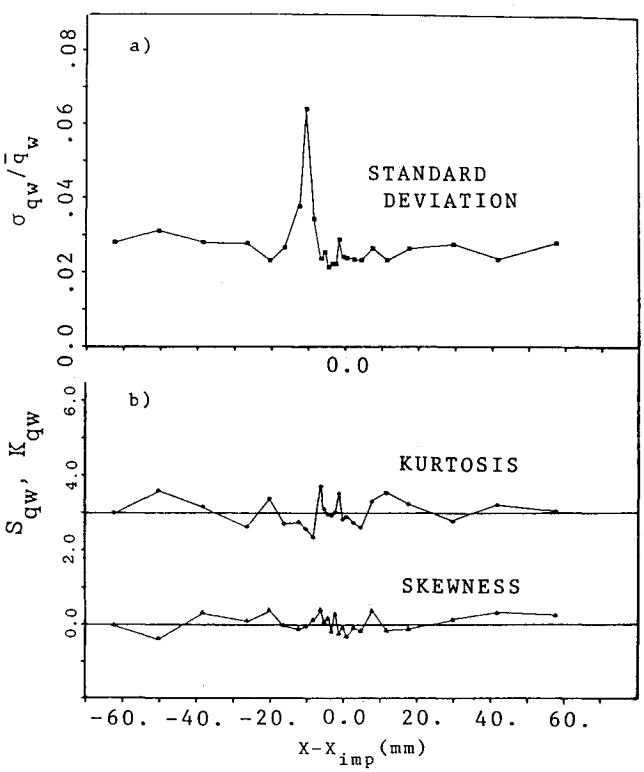

Fig. 6 a) Standard deviation and b) higher-order moments distribution of fluctuations in the unseparated interaction.

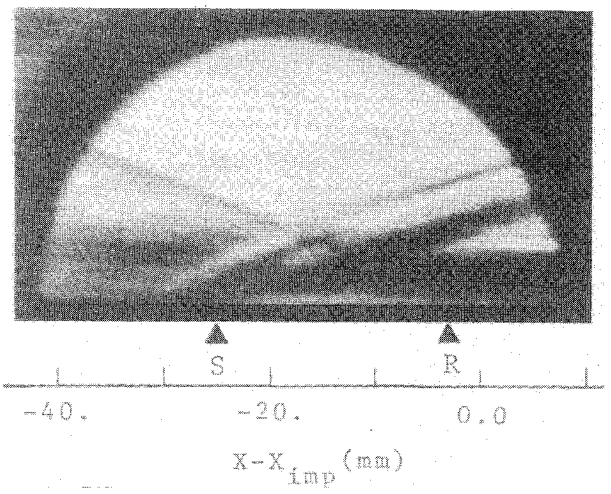

Fig. 7 Schlieren photograph of the separated interaction region.

separation point at first, then a small peak in the separated region, and a third peak near the reattachment point. The appearance of a sharp peak near the separation point is similar to that of the pressure fluctuations reported by Dolling and Murphy[9] for the case of a compression corner. The first large peak of $\sigma_{qw}/\bar{q}_w$ is considered owing to the large oscillatory motion of the separation shock. The existence of a second peak in the separated region is considered because of the incident shock wave. The values of the standard deviation downstream of the interaction region are higher than those upstream. This result implies that the fluctuations of heat flux are amplified through the separation and the reattachment of the turbulent boundary layer.

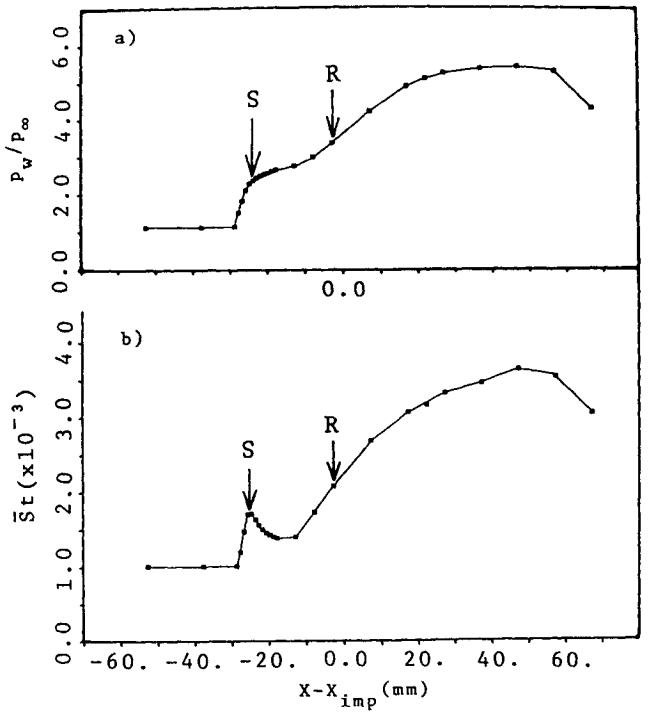

Fig. 8 a) Wall pressure and b) heat-transfer distribution in the separated interaction.

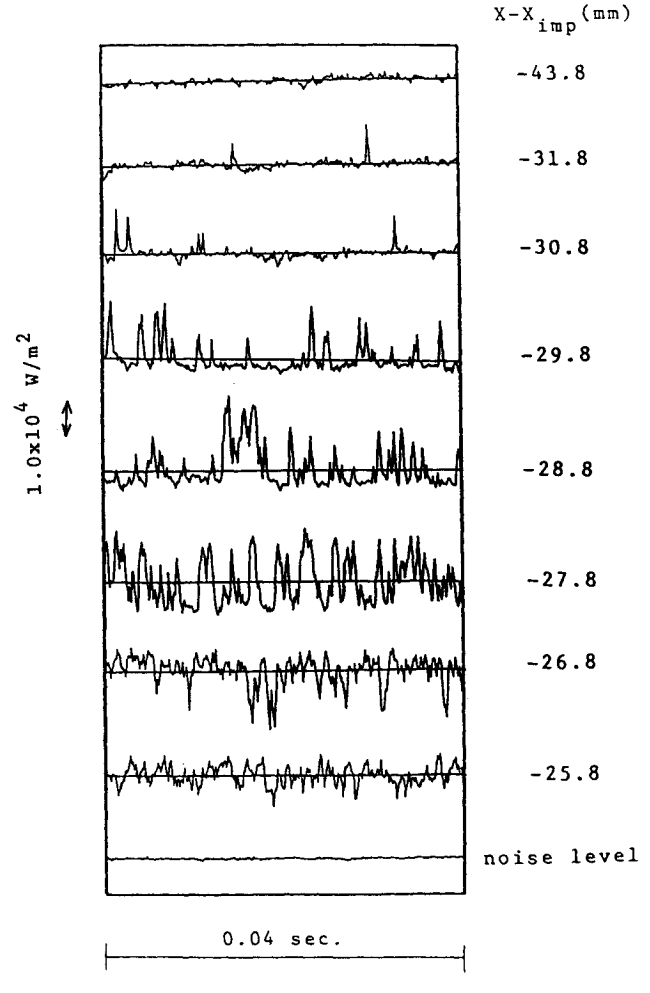

Fig. 9 Signals of the heat flux in the separated interaction.

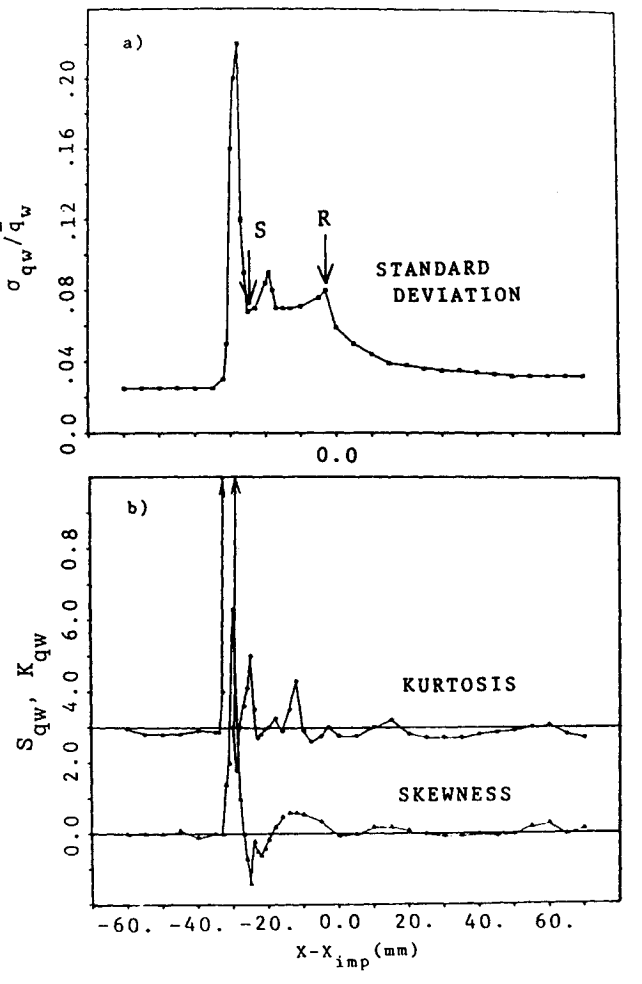

Fig. 10 a) Standard deviation and b) higher-order moments distribution of fluctuations in the separated interaction.

The wall pressure fluctuation measurement[12] also shows three peaks at nearly the same locations in the standard deviation distributions, instead of two as in Dolling and Murphy's compression corner case.[9]

The higher moments of fluctuation of heat flux are shown in Fig. 10b. Both have a large peak before the separation point. Except for the neighborhood of the separation point, the values of the higher moments are close to the Gaussian values.

The intermittent phenomena are observed before the separation point, much as in the compression corner case.[9] The representative time histories of fluctuating heat flux at $X-X_{imp} = -31.8--25.8$ mm are shown in Fig. 9. A close-up of it at $X-X_{imp} = -29.8$ mm is shown in Fig. 11. The disturbed level and the undisturbed level are predicted in this figure. The heat flux fluctuates intermittently at the undisturbed level or the disturbed level. The disturbed level appears more frequently downstream, and no intermittency is observed downstream of $X - X_{imp} = -25.8$ mm. As Dolling and Murphy pointed out,[9] this intermittent phenomenon is a remarkable feature of the separated interactions between shock waves and turbulent boundary layers. The wall pressure also showed comparable intermittency in the same region, and the disturbed levels appear with nearly the same frequency at the same locations. This intermittent phenomenon is considered the consequence of the large-scale shock system oscillations.

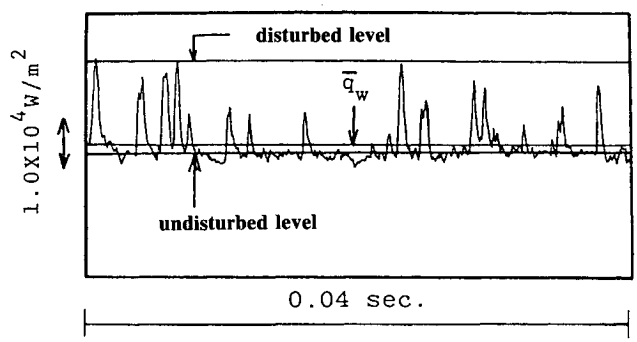

Fig. 11 Intermittent signals of heat flux at $X-X_{imp} = -29.8$ mm in the separated interaction.

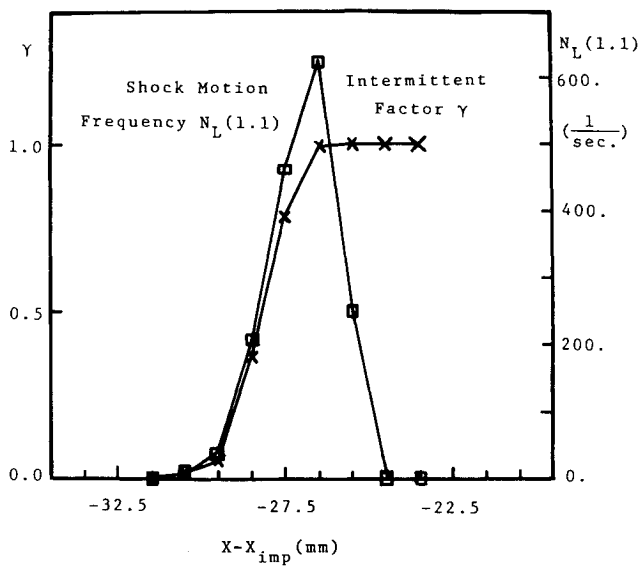

Fig. 12 Intermittent factor and shock motion frequency in the separated interaction.

The streamwise distribution of the intermittent factor γ is defined as

$$\gamma = \frac{\text{time}[q_w > (\bar{q}_{w0} + 3\sigma_{qw0})}{\text{total time}} \tag{5}$$

which represents the fraction of time the flowfield is disturbed, is shown in Fig. 12. The length of the intermittent region, where γ changes from nearly 0 to 1.0, is about 7 mm. Also the shock motion frequency $N_L(1.1)$, defined as in Ref. 9, is indicated for comparative purposes. It is defined as the number of crossings per second of the 1.1 q_{w0} level. The maximum shock motion frequency is about 620 Hz. This is about half, as in Dolling and Murphy's compression case. The cause of such discrepancy is not clear at this point, and the factors that dominate these properties must be determined with further experiments under a wide range of test conditions.

Concluding Remarks

A new heat-transfer measurement method is applied in the oblique shock wave/turbulent boundary-layer interaction regions, and the unsteadiness of heat transfer in the interaction regions has been studied. The results of the present experiments are summarized as follows:

1) When the boundary layer does not separate, deviation of the fluctuation of heat flux shows a sharp peak at the impinging point of the shock wave, and no intermittency is observed.

2) When the boundary layer separates, remarkable fluctuations of heat flux exist in the entire interaction region. The deviation has a large peak near the separation point and two peaks in the interaction region. Deviation of fluctuations is amplified downstream of the interaction region through the separation and reattachment of the boundary layer.

3) Near the separation point, intermittency of the fluctuations of heat transfer is observed because of the separation shock wave oscillations.

References

[1]Korkegi, R. H., "Survey of Viscous Interaction Associated with High Mach Number Flight, *AIAA Journal,* Vol. 9, May 1971, pp. 771-784.

[2]Holden, M. S., "Shock Wave-Turbulent Boundary Layer Interaction in Hypersonic Flow," AIAA Paper 72-74, Jan. 1972.

[3]Johnson, C. B. and Kaufman II, L. G., "Interference Heating from Interactions of Shock Waves with Turbulent Boundary Layers at Mach 6," NASA TN D-7649, Sept. 1974.

[4]Back, L. H. and Cuffel, R. F., "Shock Wave/Turbulent Boundary Layer Interactions with and without Surface Cooling," *AIAA Journal,* Vol. 14, April 1976, pp. 526-532.

[5]Hung, F. T., Greenschlag, S. N., and Scottoline, C. A., "Shock-Wave-Boundary-Layer Interactions Effects on Aerodynamic Heating," *Journal of Spacecraft and Rockets,* Vol. 14, Jan. 1977, pp. 25-31.

[6]Hayashi, M., Aso, S., and Tan, A., "Unsteady Aerodynamic Heating Phenomena in the Interaction of Shock Wave/Turbulent Boundary Layer," *Memoirs of the Faculty of Engineering, Kyushu University,* Vol. 47, Dec. 1987, pp. 231-239.

[7]Hayashi, M., Sakurai, A., and Aso, S., "A Study of a Multi-Layered Thin Film Heat Transfer Gauge and a New Method Measuring Heat Transfer Rate with It," *Transactions of the Japan Society for Aeronautical and Space Sciences,* Vol. 30, No. 88, 1987, pp. 91-101.

[8]Hayashi, M., Sakurai, A., and Aso, S., "Measurements of Heat-Transfer Coefficients in the Interaction Regions between Oblique Shock Waves and Turbulent Boundary Layers with a Multi-Layered Thin Film Heat Transfer Gauge," *Transactions of the Japan Society for Aeronautical and Space Sciences,* Vol. 30, No. 88, 1987, pp. 102-110.

[9]Dolling, D. S. and Murphy, M. T., "Unsteadiness of the Separation Shock Wave Structure in a Supersonic Compression Ramp Flowfield," *AIAA Journal,* Vol. 21, Sept. 1983, pp. 1628-1634.

[10]Kistler, A. L., "Fluctuating Wall Pressure under a Separated Supersonic Flow," *Journal of the Acoustical Society of America,* Vol. 36, March 1964, pp. 543-550.

[11]Dolling, D. S. and Bogdonoff, S. M., "An Experimental Investigation of the Unsteady Behavior of Blunt Fin-Induced Shock Wave Turbulent Boundary Layer Interactions," AIAA Paper 81-1287, June 1981.

[12]Hayashi, M., Aso, S., and Tan, A., "Fluctuations of Wall Pressure in the Interacting Region of Oblique Shock Wave and Turbulent Boundary Layer," *Technology Reports of the Kyushu University,* Vol. 59, No. 1, 1986, pp. 75-82 (in Japanese).

[13]Green, J. E., "Reflexion of an Oblique Shock Wave by a Turbulent Boundary Layer," *Journal of Fluid Mechanics,* Vol. 40, Pt. 1, 1970, pp. 81-95.